CRYSTAL GROWTH & DESIGN

Article

Cite This: Cryst. Growth Des. XXXX, XXX, XXX−XXX

pubs.acs.org/crystal

Substituent Electronegativity and Isostructurality in the Polymorphism of Clonixin Analogues

Meng Liu,[†] Guowen Shen,[‡] Zhong Yuan,[§] Sean Parkin,[∥] Faquan Yu,[†] Mingtao Zhang,[‡] Sihui Long,*[,†] and Tonglei Li*[,⊥]

[†]Key Laboratory for Green Chemical Process of Ministry of Education, Hubei Key Laboratory of Novel Reactor and Green Chemical Technology, School of Chemical Engineering and Pharmacy, Wuhan Institute of Technology, Wuhan, Hubei, China

[‡]Computational Center for Molecular Science, College of Chemistry, Nankai University, Tianjin, China

[§]Department of Medicinal Chemistry, School of Pharmaceutical Sciences, Central South University, Changsha, Hunan, China

[∥]Department of Chemistry, University of Kentucky, Lexington, Kentucky 40506, United States

[⊥]Department of Industrial and Physical Pharmacy, Purdue University, West Lafayette, Indiana, United States

Supporting Information

ABSTRACT: To gain understanding of how the variation in local weak interactions influences intermolecular interactions and subsequent crystal packing, four analogues of 2-(3-chloro-2-methyl-phenylamino)-nicotinic acid [clonixin] were synthesized by replacing the chlorine with fluorine (**1**), bromine (**2**), iodine (**3**), and hydrogen (**4**). Compounds **1**, **2**, and **3** were found to be polymorphic as shown by the discovery of two forms for each (**1-I**, **1-II**; **2-I**, **2-II**; and **3-I**, **3-II**, respectively), while compound **4** has only a single identified form. Similar to clonixin, the analogue molecules in their crystals are associated either by the acid−acid dimer homosynthon or the acid−pyridine heterosynthon, depending on the dihedral angle between the two aromatic rings. Moreover, forms **2-I**, **2-II**, **3-I**, and **3-II** are isostructural to clonixin forms **I** and **IV**, compound **4** is isostructural to compound **1** form **I**, and **2-II** is structurally similar to clonixin form **II**. The phase behaviors of these polymorphic systems were studied by differential scanning calorimetry, and it was found that **2-II** converted into **2-I** when heated, **3-II** transformed into **3-I** upon heating, and **1-II** underwent transition into **1-I**. Quantum mechanical calculations including conformational energy, hydrogen-bonding strength, lattice energy, and molecular contact were performed to provide further insight into the polymorphism. Given that all halogen derivatives are polymorphic, while the hydrogen analogue (**4**) is not, our study highlights the importance of intermolecular interactions in determining crystal packing.

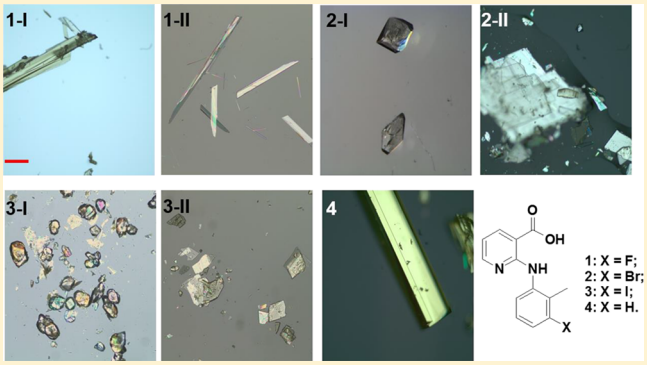

1. INTRODUCTION

[2-(2-Methyl-3-chloroanilino)nicotinic acid [clonixin or CLX] (Scheme 1) is a nonsteroidal anti-inflammatory drug (NSAID) used to treat inflammation in rheumatism, osteoporosis, collagen diseases, bursitis, and gout.[1] It also exhibited platelet-inhibitory effects,[2,3] and recently it was found to be effective for the treatment of acute migraine.[4,5] Like most classic NSAIDs, it is a nonselective cyclooxygenase (COX) inhibitor and causes side effects such as ulcer.

CLX is a conformationally flexible multifunctional molecule with two aromatic rings (one nicotinic acid, and the other disubstituted benzene) bridged by NH. Because of conformational flexibility and participation of hydrogen bonding by different functional groups, the molecule forms different polymorphs in the solid state.[6,7] Its polymorphic forms and one solvate were fully characterized by a series of spectroscopic and spectrometric methods such as powder X-ray diffraction (PXRD), Fourier transform infrared (FT-IR), Raman, and solid-state NMR, as well as theoretical approaches.[8,9]

Scheme 1

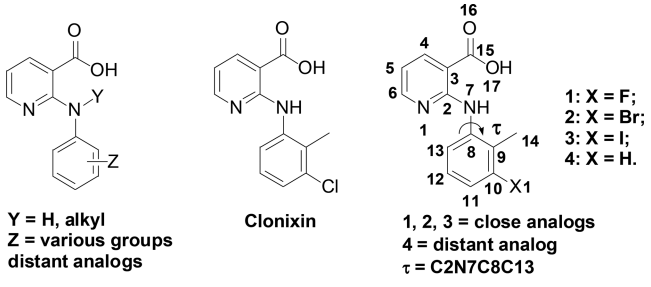

Received: August 6, 2018
Revised: September 16, 2018
Published: October 1, 2018

DOI: 10.1021/acs.cgd.8b01180
Cryst. Growth Des. XXXX, XXX, XXX−XXX

We studied several 2-anilinonicotinic acid compounds that are structurally similar to CLX. Many of these systems are highly polymorphic: for example, 2-(phenylamino)nicotinic acid [2-PNA] and 2-[methyl(phenyl)amino]nicotinic acid (2-MPNA) are, since each has four forms obtained so far.[10,11] We showed that, by chemically conjugating substituent groups to the benzene ring or alkylating the H on the bridging N, we could induce a diarylamine to take on a nonplanar conformation between the two aromatic rings leading to the acid−pyridine hydrogen-bonding chain motif[12,13] or to maintain a planar conformation leading to the acid−acid dimer motif.[14] In addition, a sandwich conformation between the twisted phenyl ring and carboxyl group leads to both acid−acid and acid−pyridine hydrogen-bonding motifs in the crystal.[15] These studies demonstrated that intermolecular interactions, both strength and pattern, are mutually influenced by the molecular conformation. Because these molecules have both carboxyl and pyridinyl N, they can associate by either the acid−acid or the acid−pyridine hydrogen bonding. Formation of a specific motif is mainly determined by the conformation and the diversity in conformational change, and hydrogen-bonding motif contributes to the polymorphism of these molecules. In addition, we studied the polymorphism of tolfenamic acid, in which the molecule only has the carboxyl but no pyridinyl N, and we found that the polymorphism is still determined by a mutual regulation of the hydrogen-bonding strength and molecular conformation.[16]

In this study, we prepared several new analogues of CLX by replacing Cl with other halogens (F, Br, and I; Scheme 1). We also compared them with the crystal structure of the hydrogen analogue (**4**).[12] Because the halogens differ subtly in electronegativity and atomic size, it would be interesting to further explore the impact of molecular interactions on crystal packing. As a diarylamine, CLX attributes its polymorphism to the interplay between energetically different planar and nonplanar conformers and relative strengths of the acid−acid and acid−pyridine hydrogen-bonding motifs. It is expected that the same tug-of-war should apply in the new systems. In addition, isostructurality and electronegativity of the halogen/hydrogen substituents could tilt the balance of forces, resulting in particular polymorphism of each compound. A variety of solvents with apolar, protic, and polar aprotic characteristics was used for the crystal growth of the CLX analogues to obtain possible polymorphs/solvatomorphs. The solid forms were fully characterized by single-crystal X-ray diffraction, FT-IR and Raman spectroscopies, and differential scanning calorimetry (DSC). The molecular structure-polymorphism relationship was analyzed both experimentally and theoretically, providing insight on the impact of each substituent.

2. EXPERIMENTAL SECTION

2.1. Materials. All chemicals were purchased from commercial sources. 2-Chloronicotinic acid and *p*-toluenesulfonic acid were from Aladdin Industrial Corporation; pyridine and other solvents were from Sinopharm Chemical Reagent Co., Ltd., and were used as received; *o*-toluidine was from Sinopharm Chemical Reagent Co., Ltd.; 3-bromo-2-methylaniline and 3-fluoro-2-methylaniline were from Energy Chemical Co., Ltd.; and 3-iodo-2-methylaniline was from Shuya Chemical Science and Technology.

2.2. Synthesis. Clonixin analogues were synthesized according to a reported method (Scheme 2).[17,18] Details of synthesis steps can be found in the Supporting Information.

2.3. Crystal Growth. Crystallization of each compound was performed in selected organic/aqueous solvents. Typically, a compound was dissolved in a given solvent to form a saturated solution at room temperature. Then the solution was set for slow evaporation, until single crystals were harvested with or without solvent remaining.[19] All crystallization experiments were conducted in the ambient atmosphere. An example is given by the following: 50 mg of compound **1** was dissolved in 10 mL of high-performance liquid chromatography (HPLC)-grade methanol in a glass vial at room temperature. The vial was covered with perforated Parafilm. Crystals were obtained as yellow plates in approximately one week. Two forms were produced for each of compounds **1**, **2**, and **3**. Only one crystal form was obtained for compound **4** in the solvents tested.

Scheme 2. Synthesis of CLX Analogues

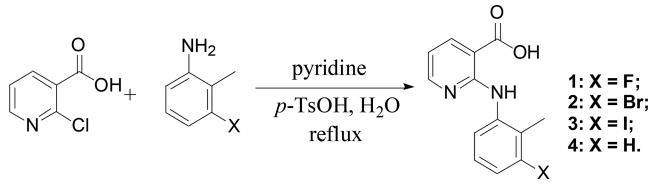

2.4. Crystal Structure Determination. Crystal structures of the synthesized analogues of CLX were determined by single-crystal X-ray diffraction. Data collection was performed at 90 K on a Nonius kappaCCD diffractometer with Mo Kα radiation (λ = 0.710 73 Å).[20] Cell refinement and data reduction were done using SCALEPACK and DENZO-SMN. Structure solution and refinement were performed using the SHELXS and SHELXL programs, respectively.[21,22]

PXRD data for each sample were collected on a Rigaku X-ray diffractometer with Cu Kα radiation (40 kV, 40 mA, λ = 1.5406 Å) between 5.0−50.0° (2θ) at ambient temperature. The finely ground sample was placed on a quartz plate in an aluminum holder prior to measurement.

2.5. Thermal Analyses. Phase behavior of the solid forms was studied by DSC. The experiments were performed on TA Instruments DSCQ20-1250. Tzero pans and aluminum hermetic lids were used at a heating rate of 10 °C/min to measure a few milligrams of sample.

2.6. Spectroscopic Measurement. IR spectra were recorded of a sample dispersed in KBr pellets using a PerkinElmer FT-IR spectrometer, while Raman spectra were recorded of a sample compressed in a gold-coated sample holder using a Thermo Raman confocal microscope.

2.7. Computation. To shed light on the polymorphism of the derivatives, we performed a series of theoretical calculations, including energy difference between planar and nonplanar conformers of each compound, strength of the acid−acid dimer and the acid−pyridine hydrogen bonds, and lattice energies of CLX analogues. In addition, conformational energy scans were conducted for each compound to identify low-energy conformers. Molecular contacts in each crystal form were examined by Hirshfeld surface analyses.[23,24]

The planar and nonplanar conformations were optimized at B3LYP/6-311g(d,p)[25,26] level based on the molecular structures in crystals. All optimizations were performed without any geometrical constraints. Frequency calculations were performed for all stationary points at the same level to identify the minima (zero imaginary frequency). The hydrogen-bond strength was evaluated of the exact structures in the crystals at m062x[27]/def2tzvp[28] level with consideration of dispersion energy. The basis set superposition error (BSSE) was accounted for by the counterpoise method.[29] The energy scan of the dihedral angle between the aromatic rings was conducted at B3LYP/6-311g(d,p) level in steps of 10°.

To calculate lattice energy, a crystal structure was first optimized at the PW1PW/POB-TZVP[28] level with the lattice parameters kept the same as the experimental values using Crystal14.[30] Dispersion energy contributions were included by the DFT-D3 program of Grimme with Becke-Johnson damping.[31,32] The BSSE was considered. The energy convergence was set to 1×10^{-7} hartree, and the root-mean-square (RMS) values of convergence were set to 0.0003 and 0.0012 au for

DOI: 10.1021/acs.cgd.8b01180
Cryst. Growth Des. XXXX, XXX, XXX−XXX

the energy gradient and atomic displacement, respectively. All calculations were conducted on a Linux cluster.

3. RESULTS AND DISCUSSION

3.1. Crystal Structures. Two forms (**1-I** and **1-II**; **2-I** and **2-II**; **3-I** and **3-II**) were discovered for each of compounds **1**−**3**, and one form was found for **4** (Figure 1). Form **1-I** crystals

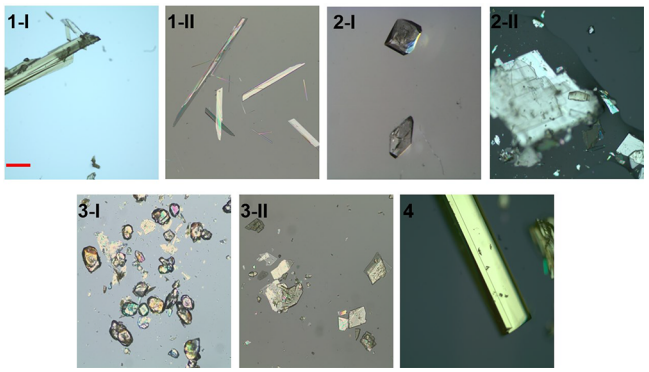

Figure 1. Crystals of the polymorphs of clonixin analogues. Scale bar: 0.2 mm.

were obtained as yellow plates from methanol (MeOH), ethyl acetate (EtOAc), ethanol (EtOH), dimethyl sulfoxide (DMSO), *N*,*N*-dimethylformamide (DMF), dichloromethane (DCM), acetonitrile (CH_3CN), chloroform ($CHCl_3$), tetrahydrofuran (THF), ether (Et_2O), or acetic acid (CH_3COOH); form **1-II** crystals were grown as light yellow needles from water (H_2O); **2-I** crystals were harvested as colorless blocks from ethanol, isopropyl alcohol (*i*-PrOH), ether, DMF, DMSO, DCM, THF, or MeOH, and **2-II** crystals were obtained as light yellow plates from ethyl acetate or acetone (CH_3COCH_3); **3-I** formed as colorless blocks from ethanol, and **3-II** formed as colorless plates from acetone; **4** grew as yellow elongated blocks from all the solvents used. The crystallization results are summarized in Table 1. Structure determination by single-crystal X-ray diffraction found forms **1-I**, **1-II**, **2-I**, **3-I**, and **4** to be of monoclinic, space group $P2_1/c$ ($Z = 4$); **2-II** and **3-II** were triclinic, space group $P\bar{1}$ ($Z = 2$). Crystallographic data of the forms are listed in Table 2; for complete CIF files, see the Supporting Information. The two crystallographically independent molecules in the two forms of **1** are conformers that differ in the dihedral angle between the two aromatic rings (7.28(5)° in **1-I** and 38.93(7)° in **1-II**). The same conformational polymorphism can be observed in compounds **2** and **3** as well (67.24(3)° in **2-I** and 1.69(8)° in **2-II**; 68.45(8)° in **3-I** and 1.97(8)° in **3-II**). Superposition of the molecules in the corresponding forms clearly reveals the main conformational difference (Figure 2). The molecule in the crystal of compound **4** is nearly flat, as shown by the dihedral angle of 2.51(3)°.

Table 1. Crystal Growth of Compounds 1−4 in Different Solvents

solvent	method	form			
acetone	slow evaporation	**1-I**	**2-II**	**3-II**	**4**
chloroform	slow evaporation	**1-I**	**2-I**		**4**
ethyl acetate	slow evaporation	**1-I**	**2-II**	**3-I** &**-3-II**	**4**
methanol	slow evaporation	**1-I**	**2-I**	**3-I** &**-3-II**	**4**
dichloromethane	slow evaporation	**1-I**	**2-I**		**4**
ethanol	slow evaporation	**1-I**	**2-I**	**3-I**	**4**
acetonitrile	slow evaporation	**1-I**			**4**
ether	slow evaporation	**1-I**	**2-I**		**4**
isopropyl alcohol	slow evaporation	**1-I**	**2-I**	**3-I** &**-3-II**	**4**
dimethyl sulfoxide	slow evaporation	**1-I**	**2-I**		**4**
tetrahydrofuran	slow evaporation	**1-I**	**2-I**		**4**
acetic acid	slow evaporation	**1-I**			**4**
DMF	slow evaporation	**1-I**	**2-I**		**4**
water	slow evaporation	**1-II**		**3-I**	**4**
benzene	slow evaporation				
toluene	slow evaporation				
pet ether	slow evaporation				
hexane	slow evaporation				

All crystal forms have one molecule in the asymmetric unit ($Z' = 1$). On the one hand, for **1**, **2**, and **3**, the polymorphism clearly results from the interplay between intramolecular interactions, manifested by the conformation, and intermolecular interactions. In **1-I**, the molecule takes a nearly planar conformation, forming the acid−acid hydrogen-bonding homosynthon ($R_2^2(8)$ in graph set notation,[33−35] Figure 3a) with the bond length and angle being 1.794 Å and 175.85°, respectively. The molecule in **1-II**, on the other hand, bears a nonplanar conformation, and the proton transfers from the carboxyl to pyridine N and causes subsequent intermolecular carboxylate-pyridinium NH hydrogen bonding with the bond length and angle being 1.868 Å and 153.63°, respectively. Molecules in **1-II** are zwitterionic and form one-dimensional (1-D) hydrogen-bonded chains (Figure 3b). The link between conformation and intermolecular hydrogen-bonding motif agrees with the general rule established in our recent study regarding the formation of either the acid−acid homosynthon or the acid−pyridine heterosynthon in 2-PNA analogues, that is, when the dihedral angle between the pyridine ring and the phenyl ring is less than 30°, the acid−acid homosynthon forms; otherwise, the acid−pyridine heterosynthon appears.[14] The dihedral angles in **1-I** and **1-II** are 7.28 (5)° and 38.93 (7)°, respectively. In addition, both forms bear an intramolecular hydrogen bond between the NH bridging the two aromatic rings and the carbonyl O (S6). The bond distance and angle are 1.940 Å and 139.97° in **1-I** and 1.827 Å and 142.19° for **1-II**. Interestingly, neither form seems to resemble any forms of CLX.

Similar observations can be made for compounds **2** and **3** as well. In **2-I**, the only molecule in the asymmetric unit is highly twisted, and the aforementioned dihedral angle is 67.24(3)°. The crystal structure is disordered at the phenyl ring. Not surprisingly, the molecules are connected through acid−pyridine heterosynthon (C6), forming one-dimensional chains parallel to the *b* axis. The hydrogen bond parameters are 1.870 Å and 171.28°, and those of the intramolecular hydrogen bond are 1.938 Å and 134.85° (Figure 4). **2-I** is similar to the form **I** of CLX. Unlike **2-I**, the molecule of **2-II** is almost flat, and the dihedral angle is 1.69(8)°. As expected, the molecules pair up via the acid−acid homosynthon. The parameters of the inter- and intramolecular hydrogen bond are 1.856 Å and 171.81°, and 1.924 Å and 140.59°, respectively (Figure 4). **2-II** resembles the form **IV** of CLX. In **3-I**, the molecule is highly twisted, as indicated by its dihedral angle of 68.45(8)°. Both aromatic rings are disordered. Because of the nonplanarity, a 1-D acid−pyridine hydrogen-bonding chain is formed (Figure 5). The parameters of the intermolecular and intramolecular hydrogen bonds are, respectively, 1.863 Å and 167.59°, and

DOI: 10.1021/acs.cgd.8b01180
Cryst. Growth Des. XXXX, XXX, XXX−XXX

Table 2. Crystallographic Data of Compounds 1−4

	1-I	1-II	2-I	2-II	3-I	3-II	4
formula	$C_{13}H_{11}FN_2O_2$	$C_{13}H_{11}FN_2O_2$	$C_{13}H_{11}BrN_2O_2$	$C_{13}H_{11}BrN_2O_2$	$C_{13}H_{11}IN_2O_2$	$C_{13}H_{11}IN_2O_2$	$C_{13}H_{12}N_2O_2$
formula weight	246.24	246.24	307.15	307.15	354.14	354.14	228.25
crystal size	0.40 × 0.15 × 0.02	0.40 × 0.10 × 0.05	0.30 × 0.25 × 0.20	0.35 × 0.30 × 0.02	0.30 × 0.20 × 0.10	0.40 × 0.20 × 0.05	0.45 × 0.10 × 0.10
crystal system	monoclinic	monoclinic	monoclinic	triclinic	monoclinic	triclinic	monoclinic
space group	$P2_1/c$	$P2_1/c$	$P2_1/c$	$P\bar{1}$	$P2_1/c$	$P\bar{1}$	$P2_1/c$
a, Å	3.821(1)	3.85100(10)	7.605(1)	7.646(1)	7.8162(16)	7.10120(10)	4.933(1)
b, Å	21.056(4)	22.3090(6)	14.106(2)	7.098(1)	14.053(3)	7.69820(10)	21.146(4)
c, Å	13.791(3)	12.5920(4)	11.762(2)	11.050(2)	12.023(2)	11.5625(2)	10.378(2)
α, deg	90	90	90	100.32(1)	90	78.6401(7)	90.00
β, deg	96.01(1)	92.4090(10)	101.82(1)	101.36(1)	103.05(3)	79.5043(7)	97.10(1)
γ, deg	90	90	90	87.46(1)	90	86.5626(7)	90.00
Z, Z'	4, 1	4, 1	4, 1	2, 1	4,1	2,1	4,1
V, Å^3	1103.5(4)	1080.85(5)	1235.0(3)	578.41(15)	1286.5(4)	609.140(16)	1074.3(4)
D_{cal}, g cm^{-3}	1.482	1.513	1.652	1.764	1.828	1.931	1.411
T, K	90(2)	90(2)	90 (2)	90 (2)	90(2)	90(2)	90(2)
abs coeff (mm^{-1})	0.113	0.115	3.323	3.548	2.484	2.624	0.097
F(000)	512.0	512.0	616.0	308.0	688	344	480
θ range, deg	1.77−27.41	1.83−27.45	2.28−27.49	1.91−27.50	2.26−27.47	1.82−27.48	2.20−27.49
limiting indices	$-4 \le h \le 4$	$-4 \le h \le 4$	$-9 \le h \le 9$	$-9 \le h \le 9$	$-10 \le h \le 10$	$-9 \le h \le 9$	$-6 \le h \le 6$
	$-27 \le k \le 27$	$-28 \le k \le 28$	$-18 \le k \le 16$	$-9 \le k \le 9$	$-18 \le k \le 18$	$-9 \le k \le 9$	$-27 \le k \le 27$
	$-17 \le l \le 17$	$-16 \le l \le 16$	$-15 \le l \le 15$	$-14 \le l \le 14$	$-15 \le l \le 15$	$-14 \le l \le 15$	$-13 \le l \le 13$
completeness to 2θ	100%	100%	100%	99.8%	99.7%	99.7%	99.8%
unique reflections	1701	1504	2310	2124	2420	2651	1852
R_1 [$I > 2\sigma(I)$]	0.0498	0.0526	0.0436	0.0396	0.0300	0.0280	0.0467
wR_2 (all data)	0.1289	0.1660	0.0980	0.0964	0.0652	0.0741	0.1414
CCDC code	1860257	1860258	1860259	1860260	1860261	1860262	CUNKOM

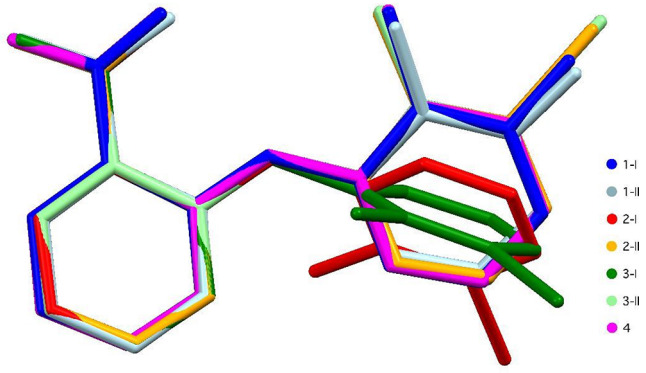

Figure 2. Superposition of molecules in the asymmetric units of the polymorphs of compounds **1**, **2**, and **3**.

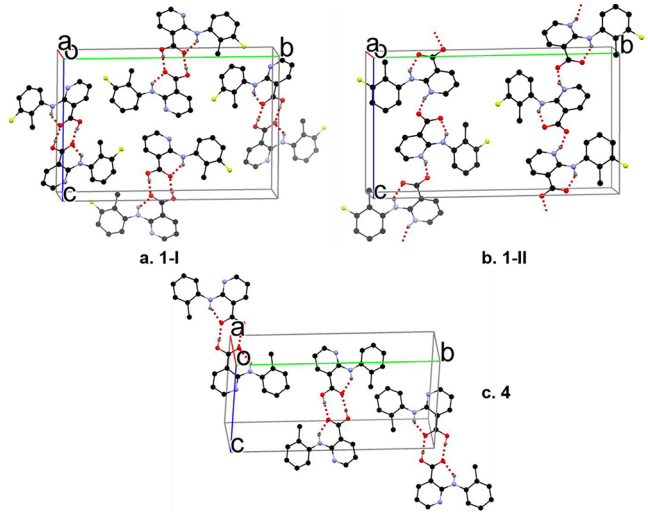

Figure 3. Crystal packing of **1-I** (a), **1-II** (b), and **4**. For clarity, only hydrogens participating hydrogen bonds are shown.

1.944 Å and 135.54°. **3-I** resembles the form **I** of CLX, while in **3-II**, the molecule is nearly flat with the dihedral angle of 1.97(8)°. Acid−acid dimers are formed as anticipated (Figure 5). The parameters are 1.862 Å and 173.27° for the intermolecular hydrogen bond, and 1.921 Å and 140.87° for the intramolecular bond. **3-II** resembles form **IV** of CLX.

Only one crystal form was obtained for compound **4**. The structure is similar to **1-I** and unlike any known form of CLX. The similarity may stem from the similar atomic size of F and H. The conformation is planar with a dihedral of 2.51(3)°. The crystal is based on dimers built on the acid−acid homosynthon (Figure 3c). The hydrogen-bond parameters are 1.801 Å and 177.71°, and 1.945 Å and 140.56° for inter- and intramolecular bonds, respectively.

Figure 6 shows PXRD patterns of individual forms of each system collected at room temperature, along with PXRD patterns calculated from the single-crystal structures determined at 90 K. The similarity between the experimental and simulated patterns indicates the thermodynamic stability at room temperature. The comparison also suggests that each batch of crystallization product had a relatively high phase purity.

3.2. Thermal Properties. Melting point and heat of fusion were measured by DSC for each system (Figure 7). **1-I** showed a single thermal event with an onset temperature of 184.3 °C,

DOI: 10.1021/acs.cgd.8b01180
Cryst. Growth Des. XXXX, XXX, XXX−XXX

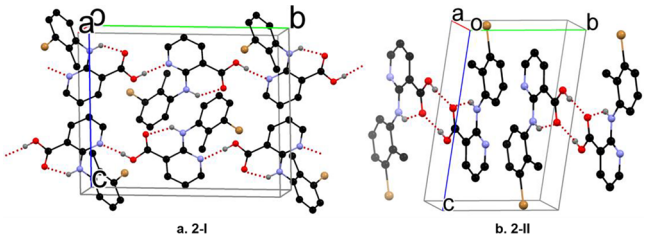

Figure 4. Crystal packing of **2-I** (a) and **2-II** (b). For clarity, only hydrogens participating hydrogen bonds are shown.

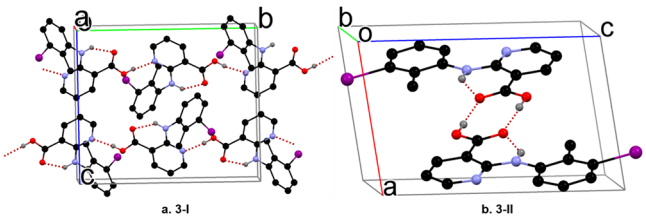

Figure 5. Crystal packing of **3-I** (a) and **3-II** (b). For clarity, only hydrogens participating hydrogen bonds are shown.

which corresponds to melting. **1-II** displayed at least two thermal events. The first, at the onset temperature of 170.4 °C, corresponds to the melting of the form, followed by crystallization of the melt, as suggested by the exothermic peak. This new form is expected to be **1-I**, because its melting point matches that of **1-I** (Figure 7). The shoulder of the first melting peak may also suggest that it crystallized into another form, which then transitioned into **1-I**. **2-I** revealed two thermal events by DSC. The first had an onset temperature of 237.9 °C with a small heat of fusion of 2.4 J/g, which could be a solid−solid phase transition to a new form. This new form melted at ∼250 °C. **2-II** also showed two thermal events with

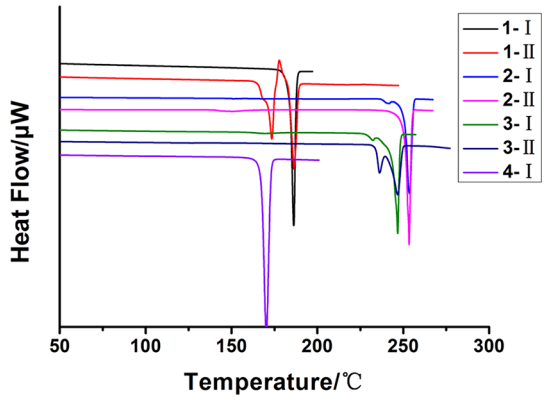

Figure 7. DSC of polymorphs of compounds **1**−**3** and the only form of compound **4**.

the first one at 141 °C, which is believed to be solid−solid phase transition into a new solid form. The new form melted at 252.0 °C (Figure 7). It seems that the new forms generated from heating of **2-I** and **2-II** could be of the same crystal form, but more experimentation is needed to characterize this new high-temperature form. The thermal behaviors of **3-I** and **3-II** also involved multiple events. **3-I** melted at 229.8 °C (heat of fusion of 11.7 J/g), followed by recrystallization to a new form, which melted at 244.5 °C. There seems to be a small peak at ∼170 °C (heat of fusion of 3.5 J/g) as well. **3-II** melted at 234.4 °C, which recrystallized into the same new form (Figure 7). Lastly, compound **4** gave only one melting peak with an onset temperature of 168.0 °C (Figure 7).

3.3. Computational Analyses. Optimization of single molecules of the compounds indicates that the neutral planar conformers are more stable than the nonplanar ones to various degrees; the energy differences span 1.5−2.2 kcal/mol (Table

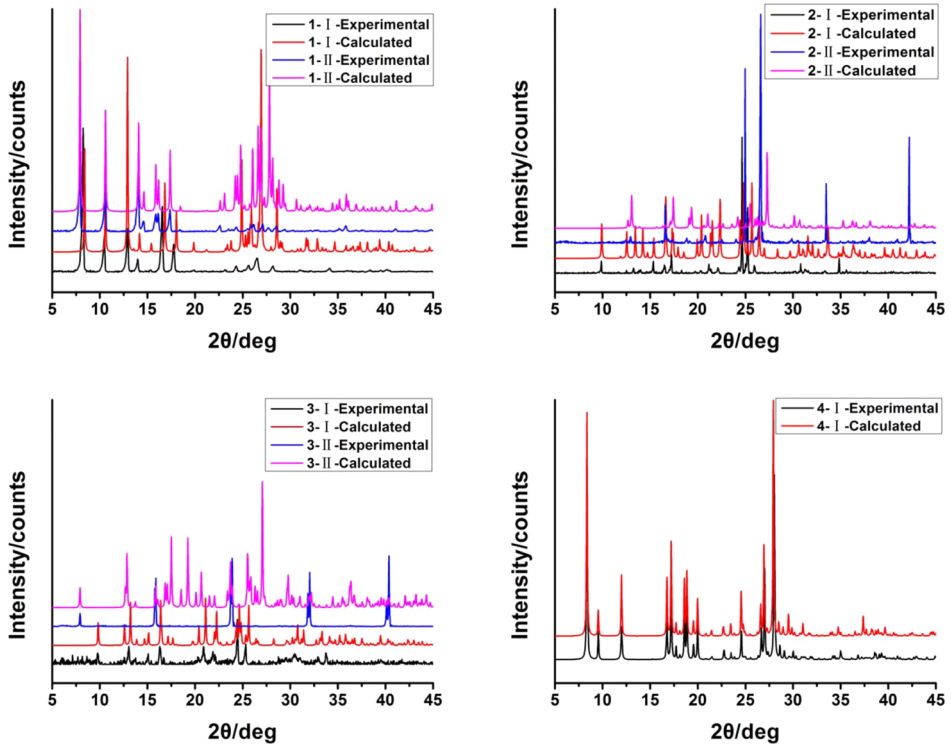

Figure 6. PXRD of polymorphs of compounds **1**−**3** and the one form of **4**.

DOI: 10.1021/acs.cgd.8b01180
Cryst. Growth Des. XXXX, XXX, XXX−XXX

Table 3. Energy Difference[a] between Planar and Nonplanar/Zwitterion Conformations of Compounds 1−4

		CLX	1	2	3	4
E (hartree)	planar	−1222.414 954	−862.060 186	−3336.334 895	−7681.714 188	−762.794 924
	nonplanar	−1222.412 646	−862.057 174	−3336.332 655	−7681.712 187	−762.792 084
	zwitterion		−862.042 685			
E0 (hartree)	planar	−1222.195 247	−861.839 094	−3336.115 946	−7681.495 705	−762.565 777
	nonplanar	−1222.193 504	−861.836 616	−3336.114 178	−7681.494 045	−762.563 477
	zwitterion		−861.822 422			
G (hartree)	planar	−1222.239 784	−861.882 541	−3336.162 566	−7681.543 637	−762.608 556
	nonplanar	−1222.237 647	−861.879 885	−3336.159 436	−7681.540 089	−762.605 590
	zwitterion		−861.866 384			
Δ*G* (kcal/mol)	nonplanar soft-enter replaced as-planar	1.34	1.67	1.96	2.23	1.86
Δ*G* (kcal/mol)	zwitterion-planar		10.14			

[a]Gibbs free energies were calculated under 298.15 K and 1 atm.

3). The largest difference is observed for the zwitterionic and planar species of **1**, with the planar conformer 10.14 kcal/mol lower in energy than the zwitterion. Given the size similarity between F and H of **1** and **4**, the electronegative F appears to strengthen the planar conjugation between phenyl and amino groups. Our previous study did demonstrate that the presence of highly electronegative substituents on the phenyl ring could enforce a planar conformation in the diarylamine compounds.[13] The major difference in conformation stems from the dihedral angle τ, as illustrated by Figure 2. From the conformation energy scan of τ (Figure 8), similar results can be

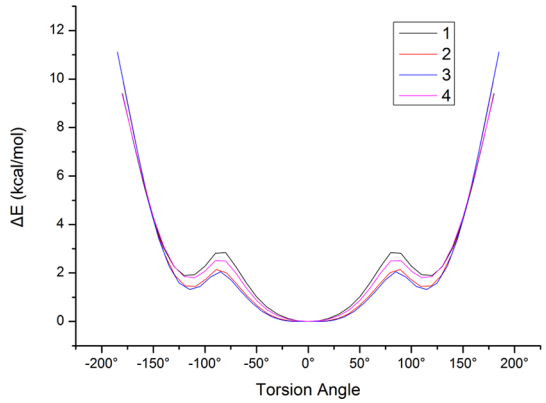

Figure 8. Relaxed potential energy surface scan for the rotation of the aniline bond ($C_2N_7C_8C_{13}$).

observed with the global minimum located at 0° and two local minima (stereochemically identical) at ±120°, ±119°, ±115°, and ±110° for **1**−**4**, with the energy barriers between the global and local minima of 3.2, 2.6, 2.1, and 2.8 kcal/mol, respectively.

Our earlier work and other related studies showed that the heterogeneous acid−pyridine hydrogen bond is energetically favored relative to the homogeneous acid−acid hydrogen bond.[36−40] In both CLX and the three compounds (**1**, **2**, and **3**) investigated, the same observation is made. The energy strengths of the acid−pyridine hydrogen bond (10.94, 10.84, and 10.80 kcal/mol of CLX-NP, **2-I**, and **3-I**) are considerably higher than those of the acid−acid hydrogen bond (6.70, 6.47, 6.53, 6.41, and 6.67 kcal/mol for CLX-P, **1-I**, **2-II**, **3-II**, and **4**). The hydrogen bond between the pyridinium NH and carboxylate in **1-II** is much stronger than the acid−pyridine hydrogen bond due to the electrostatic interaction (22.89 kcal/mol). The hydrogen-bonding strength values and corresponding motifs are summarized in Table 4. Thus, the loss of stability due to molecular nonplanarity can be compensated by

Table 4. Hydrogen Bonding Strength of Various Synthons

	intermolecular interactions (kcal/mol)	number of hydrogen bond	hydrogen bond strength (kcal/mol)	description
NP	−10.94	1	−10.94	nonplanar, acid−pyridine heterosynthon
P	−13.39	2	−6.7	planar, acid−acid homosynthon
1-I	−12.95	2	−6.47	planar, acid−acid homosynthon
1-II	−22.89	1	−22.89	nonplanar zwitterion, carboxylate−pyridinium NH heterosynthon
2-I	−10.84	1	−10.84	twisted, acid−pyridine heterosynthon
2-II	−13.06	2	−6.53	planar, acid−acid homosynthon
3-I	−10.8	1	−10.8	nonplanar, acid−pyridine heterosynthon
3-II	−12.82	2	−6.41	planar, acid−acid homosynthon
4	−13.35	2	−6.67	planar, acid−acid homosynthon

the gain from hydrogen bonding. Lattice energies for the new crystals are calculated to be −48.62 and −52.15 kcal/mol for **1-I** and **1-II**, −54.17 and −52.60 kcal/mol for **2-I** and **2-II**, −55.89 and −56.00 kcal/mol for **3-I** and **3-II**, and −47.82 kcal/mol for **4**. The overall strengths of intermolecular interactions of the polymorphs of each compound and among the compounds are generally within a few Kcal/mol, and the differences apparently result from the substitution by the halogens and hydrogen. The calculated densities are 1.482 and 1.513 g/cm^3 for **1-I** and **1-II**, 1.652 and 1.764 g/cm^3 for **2-I** and **2-II**, 1.828 and 1.931 g/cm^3 for **3-I** and **3-II**, and 1.411 g/cm^3 for **4**. For the polymorphic systems of **1** and **3**, the ordering in lattice energy is in agreement with the densities, while for **2-I** and **2-II**, the lattice energies do not match with the densities. Yet this is not a total surprise, since packing is not the only factor contributing to the lattice energy. The DSC measurement suggests that **1-I** and **2-I** are the more stable forms at higher temperature, compared with respective **1-II** and **2-II**, with the lattice energy values only echoing the two forms of **2**. It could be the zwitterionic form of **1-II** becomes less stable at elevated temperature. Interestingly, the lattice energies of **3-I** and **3-II** are almost identical, and the DSC

DOI: 10.1021/acs.cgd.8b01180
Cryst. Growth Des. XXXX, XXX, XXX−XXX

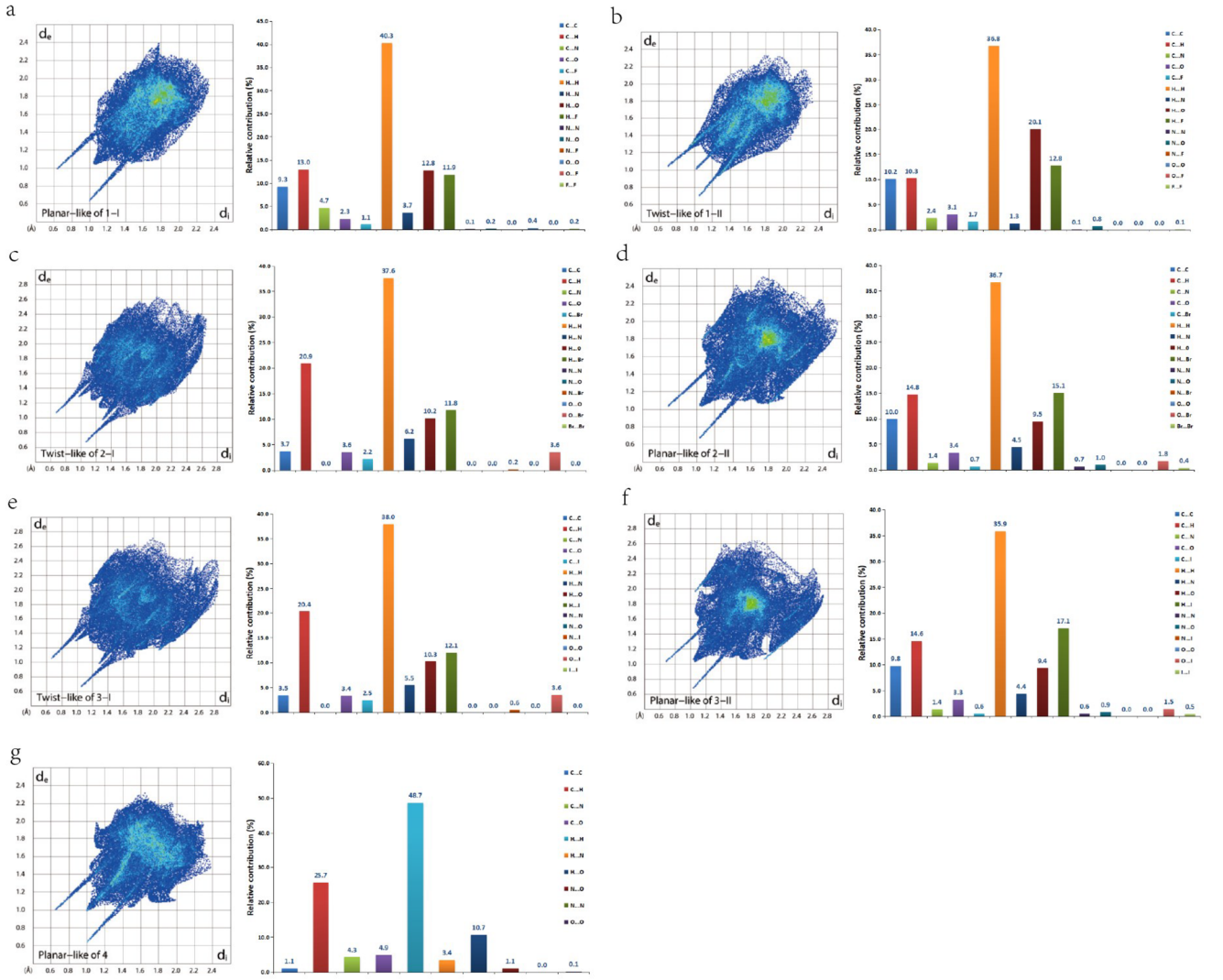

Figure 9. Fingerprint plots and relative contribution of intermolecular contacts on the base of Hirshfeld surface analysis: (a) **1-I**, (b) **1-II**, (c) **2-I**, (d) **2-II**, (e) **3-I**, (f) **3-II**, and (g) **4**.

results suggest a high-temperature form that is different from either.

Hirshfeld surface analyses further reveal intermolecular contacts of these compounds. Two-dimensional (2-D) fingerprint plots and relative contributions of various interactions by Hirshfeld surfaces were calculated for **1**–**4** (Figure 9). Contributions by the H···O contacts show significant changes from 12.8%, 9.5%, and 9.4% in **1-I**, **2-II**, **3-II** (all with planar conformations) to 20.1%, 10.2%, and 10.3% in **1-II**, **2-I**, and **3-I** (all with nonplanar conformations), respectively. These changes obviously stem from the change in the hydrogen-bonding motif, with **1-I** and **1-II** showing the largest increase, corroborating the hydrogen bonding in **1-II** being much stronger. This is further revealed by the decrease in contribution of the H···N contact from 3.7% of **1-I** to 1.3% of **1-II**, while increases are seen from 4.5% and 4.4% of **2-II** and **3-II** to 6.2% and 5.4% of **2-I** and **3-I**, respectively.

Overall, the most interesting finding of the study lies in the polymorphism of the compounds. All of the halogen derivatives are polymorphic, whereas for compound **4** only one form has been obtained. Its DSC measurement also revealed no high-temperature form. It is also intriguing that the energy difference between the planar and twisted conformers of **4** is the smallest (Table 2). It seems intuitive that **4** should be polymorphic, given that the acid–pyridine hydrogen bonding is much stronger, and a form bearing such a motif needs to overcome a smaller conformational energy barrier. In addition, kinetic factors might be ruled out, because a variety of different solvents were utilized in crystallization of these compounds. All these details suggest that secondary interactions such as $\pi-\pi$ stacking, as compared to hydrogen bonding, may further guide the molecular packing during nucleation. When the molecule remains planar, it can form much stronger $\pi-\pi$ stacking, as compared with a twisted conformation. Nuclei formed by planar conformers become more favorable energetically and continue to grow. For the halogenated clonixin derivatives (**1**, **2**, and **3**), conversely, either hydrogen-bonding motif can be realized in practice, resulting in respective polymorphs, likely because of similar energy states achieved jointly by conformation and $\pi-\pi$ stacking.

4. CONCLUSIONS

Four analogues of CLX were synthesized by replacing the chlorine with fluorine (**1**), bromine (**2**), iodine (**3**), and hydrogen (**4**), and their polymorphism was investigated.

DOI: 10.1021/acs.cgd.8b01180
Cryst. Growth Des. XXXX, XXX, XXX–XXX

Compounds **1**, **2**, and **3** were found to be polymorphic, as two forms were discovered for each, while for compound **4**, only one form was identified. Similar to CLX, the molecules in their crystals are connected either by the acid−acid dimer homosynthon or the acid−pyridine heterosynthon, depending on the dihedral angle between the two aromatic rings. Isostructurality was observed between **2-I**, **3-I** and form **I** of CLX and between **2-II**, **3-II** and form **IV** of CLX, likely due to the similar electronegativity and not significant size difference. **4** is isostructural to **1-I**, but not to the other crystals, possibly because of the size similarity between F and H and electronegativity dissimilarity between F/H and Cl, Br, and I. Phase behaviors of the polymorphic systems were studied by DSC, which showed phase transitions between the different forms in each system. Conformational energy, hydrogen-bond strength calculations, and conformation scans suggested both conformational flexibility and the possibility of multiple hydrogen-bonding motifs lead to the polymorphism of the compounds and suggest additional forms might be found for each compound. Lattice energy evaluation and Hirshfeld analysis further provided insight on the relative stability of the polymorphs of each system and contributions to the stability of each form. The lack of polymorphs of compound **4** deserves further investigation.

■ ASSOCIATED CONTENT

Supporting Information

The Supporting Information is available free of charge on the ACS Publications website at DOI: 10.1021/acs.cgd.8b01180.

Synthesis of CLX analogues; IR and Raman spectra (PDF)

Accession Codes

CCDC 1860257−1860262 contain the supplementary crystallographic data for this paper. These data can be obtained free of charge via www.ccdc.cam.ac.uk/data_request/cif, or by emailing data_request@ccdc.cam.ac.uk, or by contacting The Cambridge Crystallographic Data Centre, 12 Union Road, Cambridge CB2 1EZ, UK; fax: +44 1223 336033.

■ AUTHOR INFORMATION

Corresponding Authors

*Phone: (027) 87194980. E-mail: Sihuilong@wit.edu.cn; longsihui@yahoo.com. (S. Long)

*Phone: (765) 494-1451. E-mail:tonglei@purdue.edu. (T. Li)

ORCID

Faquan Yu: 0000-0002-5062-8731

Sihui Long: 0000-0002-4424-6374

Tonglei Li: 0000-0003-2491-0263

Notes

The authors declare no competing financial interest.

■ ACKNOWLEDGMENTS

S.L. thanks Natural Science Foundation of Hubei Province for financial support (2014CFB787). T.L. is grateful to NSF for supporting the work (DMR1006364).

■ REFERENCES

(1) Sherlock, M. H.; Sperber, N. Antiinflammatory 2-Anilinonicotinic acids. *Br. Pat. GB 1147701*, **1969**.

(2) Widmer, K.; Reed, R. C.; Freireich, E. J. The influence of a new analgetic-antiphlogistic compound (2-(2-methyl-3′chloro)-anilinonicotinic acid) on platelet function and fibrinolytic activity in vitro. *Thromb. Res.* **1975**, *6*, 9.

(3) Arkel, Y. S.; Schrogie, J. J.; Williams, R. Effect of clonixin and aspirin on platelet aggregation in human volunteers. *J. Clin. Pharmacol.* **1976**, *16*, 30.

(4) Morse, E. E. Effects of drugs on platelet function. *Ann. Clin. Lab. Sci.* **1977**, *7*, 68.

(5) Krymchantowski, A. V.; Carneiro, H.; Barbosa, J.; Jevoux, C. Lysine clonixinate versus dipyrone (metamizole) for the acute treatment of severe migraine attacks: a single-blind, randomized study. *Arq. Neuro-Psiquiatr.* **2008**, *66*, 216.

(6) Nangia, A. Conformational polymorphism in organic crystals. *Acc. Chem. Res.* **2008**, *41*, 595.

(7) Cruzcabeza, A. J.; Bernstein, J. Conformational polymorphism. *Chem. Rev.* **2014**, *114*, 2170−2191.

(8) Takasuka, M.; Nakai, H.; Shiro, M. Infrared spectral and X-Ray studies of polymorphic forms of 2-(2-methyl-3-chloroanilino)-nicotinic acid. *J. Chem. Soc., Perkin Trans. 2* **1982**, *2*, 1061.

(9) Long, S.; Mao, T. F.; Chen, P.; Liu, M.; Parkin, S.; Zhang, M.; Li, T.; Zhou, P.; Yu, F. Strong hydrogen bond leads to a fifth crystalline form and polymorphism of clonixin. *ChemistrySelect* **2017**, *2*, 4942.

(10) Long, S.; Parkin, S.; Siegler, M. A.; Cammers, A.; Li, T. Polymorphism and phase behaviors of 2-(Phenylamino)nicotinic acid. *Cryst. Growth Des.* **2008**, *8*, 4006.

(11) Long, S.; Parkin, S.; Siegler, A.; Brock, C.; Cammers, A.; Li, T. Polymorphism of an organic system effected by the directionality of hydrogen-bonding chains. *Cryst. Growth Des.* **2008**, *8*, 3137.

(12) Long, S.; Li, T. Controlled Formation of the Acid-Pyridine Heterosynthon over the Acid-Acid Homosynthon in 2-Anilinonicotinic Acids. *Cryst. Growth Des.* **2009**, *9*, 4993.

(13) Long, S.; Li, T. Enforcing molecule's π-conjugation and consequent formation of the acid-acid homosynthon over the acid-pyridine heterosynthon in 2-anilinonicotinic acids. *Cryst. Growth Des.* **2010**, *10*, 2465.

(14) Chen, P.; Zhang, Z.; Parkin, S.; Zhou, P.; Cheng, K.; Li, C.; Yu, F.; Long, S. Preferred formation of the carboxylic acid−pyridine heterosynthon in 2-anilinonicotinic acids. *RSC Adv.* **2016**, *6*, 81101.

(15) Long, S.; Zhou, P.; Parkin, S.; Li, T. From competition to commensuration by two major hydrogen-bonding motifs. *Cryst. Growth Des.* **2014**, *14*, 27.

(16) Mattei, A.; Li, T. Interplay between molecular conformation and intermolecular interactions in conformational polymorphism: A molecular perspective from electronic calculations of tolfenamic acid. *Int. J. Pharm.* **2011**, *418*, 179.

(17) Kermack, W. O.; Weatherhead, A. P. Some anilinopyridine derivatives. *J. Chem. Soc.* **1942**, 726.

(18) Ting, P. C.; Kaminski, J. J.; Sherlock, M. H.; Tom, W. C.; Lee, J. F.; Bryant, R. W.; Watnick, A. S.; McPhail, A. T. Substituted 1,3-dihydro-2H-pyrrolo[2,3-b]pyridin-2-ones as potential antiinflammatory agents. *J. Med. Chem.* **1990**, *33*, 2697.

(19) Chen, P.; Jin, Y.; Zhou, P.; Parkin, S.; Zhang, Z.; Long, S. Solid-state characterization of 2-[(2,6-dichlorophenyl)amino]-benzaldehyde: an experimental and theoretical investigation. *J. Chin. Chem. Soc.* **2017**, *64*, 531.

(20) Nonius *Collect;* Nonius BV: Delft, the Netherlands, 2002.

(21) Sheldrick, G. M. A short history of SHELX. *Acta Crystallogr., Sect. A: Found. Crystallogr.* **2008**, *64*, 112.

(22) Sheldrick, G. M. Crystal structure refinement with SHELXL. *Acta Crystallogr., Sect. C: Struct. Chem.* **2015**, *71*, 3.

(23) Hirshfeld, F. L. Bonded-atom fragments for describing molecular charge densities. *Theor. Chim. Acta* **1977**, *44*, 129.

(24) Spackman, M. A.; Jayatilaka, D. Hirshfeld surface analysis. *CrystEngComm* **2009**, *11*, 19.

(25) Becke, A. D. Density-functional thermochemistry. III. The role of exact exchange. *J. Chem. Phys.* **1993**, *98*, 5648.

(26) Krishnan, R.; Binkley, J. S.; Seeger, R.; Pople, J. A. Self-consistent molecular orbital methods. XX. A basis set for correlated wave functions. *J. Chem. Phys.* **1980**, *72*, 650.

DOI: 10.1021/acs.cgd.8b01180
Cryst. Growth Des. XXXX, XXX, XXX−XXX

(27) Zhao, Y.; Truhlar, D. G. The M06 suite of density functionals for main group thermochemistry, thermochemical kinetics, noncovalent interactions, excited states, and transition elements: two new functionals and systematic testing of four M06-class functionals and 12 other functionals. *Theor. Chem. Acc.* **2008**, *120*, 215−241.
(28) Weigend, F.; Ahlrichs, R. Balanced basis sets of split valence, triple zeta valence and quadruple zeta valence quality for H to Rn: Design and assessment of accuracy. *Phys. Chem. Chem. Phys.* **2005**, *7*, 3297−3305.
(29) Boys, S. F.; Bernardi, F. The calculation of small molecular interactions by the differences of separate total energies. Some procedures with reduced errors. *Mol. Phys.* **1970**, *19*, 553.
(30) Dovesi, R.; Orlando, R.; Erba, A.; Zicovich-Wilson, C. M.; Civalleri, B.; Casassa, S.; Maschio, L.; Ferrabone, M.; De La Pierre, M.; D'Arco, P.; Noel, Y.; Causa, M.; Rerat, M.; Kirtman, B. CRYSTAL14: A program for the ab initio investigation of crystalline solids. *Int. J. Quantum Chem.* **2014**, *114*, 1287.
(31) Grimme, S.; Antony, J.; Ehrlich, S.; Krieg, H. A consistent and accurate ab intio parameterization of density functional dispersion correction (DFT-D) for the 94 elements H-Pu. *J. Chem. Phys.* **2010**, *132*, 154014.
(32) Grimme, S.; Ehrlich, S.; Goerigk, L. Effect of the damping function in dispersion corrected density functional theory. *J. Comput. Chem.* **2011**, *32*, 1456−1465.
(33) Etter, M. C. Encoding and decoding hydrogen-bond patterns of organic compounds. *Acc. Chem. Res.* **1990**, *23*, 120.
(34) Etter, M. C.; Macdonald, J. C.; Bernstein, J. Graph-set analysis of hydrogen-bond patterns in organic crystals. *Acta Crystallogr., Sect. B: Struct. Sci.* **1990**, *46*, 256.
(35) Bernstein, J.; Davis, R. E.; Shimoni, L.; Chang, N. L. Patterns in hydrogen bonding: functionality and graph set analysis in crystals. *Angew. Chem., Int. Ed. Engl.* **1995**, *34*, 1555.
(36) Li, T.; Zhou, P.; Mattei, A. Electronic origin of pyridinyl N as a better hydrogen-bonding acceptor than carbonyl O. *CrystEngComm* **2011**, *13*, 6356.
(37) Steiner, T. Competition of hydrogen-bond acceptors for the strong carboxyl donor. *Acta Crystallogr., Sect. B: Struct. Sci.* **2001**, *57*, 103−106.
(38) Aakeröy, C. B.; Beatty, A. M.; Helfrich, B. A. "Total synthesis" supramolecular style: design and hydrogen-bond-directed assembly of ternary supermolecules. *Angew. Chem., Int. Ed.* **2001**, *40*, 3240−3242.
(39) Vishweshwar, P.; Nangia, A.; Lynch, V. M. Molecular complexes of homologous alkanedicarboxylic acids with isonicotinamide: X-ray crystal structures, hydrogen bond synthons, and melting point alternation. *Cryst. Growth Des.* **2003**, *3*, 783−790.
(40) Shattock, T. R.; Arora, K. K.; Vishweshwar, P.; Zaworotko, M. J. Hierarchy of Supramolecular Synthons: Persistent Carboxylic Acid···Pyridine Hydrogen Bonds in Cocrystals That also Contain a Hydroxyl Moiety. *Cryst. Growth Des.* **2008**, *8*, 4533−4545.

DOI: 10.1021/acs.cgd.8b01180
Cryst. Growth Des. XXXX, XXX, XXX−XXX